Clinical Ophthalmology

Dovepress
Taylor & Francis Group

Open Access Full Text Article

ORIGINAL RESEARCH

Retinal Assessment and the Retina–Choroid Link in Precapillary Pulmonary Hypertension: A Single-Center Cross-Sectional Study

Aleksandra Leoniuk[1], Katarzyna Ptaszynska[2], Anna Szwedowicz[1], Emilia Sawicka-Smiarowska[2], Remigiusz Kazimierczyk[2], Agnieszka Zonenberg[1], Barbara Pieklarz[1], Daniel Baldyga[1], Iwona Obuchowska[1], Joanna Konopinska[1], Karol A Kaminski[2], Diana A Dmuchowska[1]

[1]Department of Ophthalmology, Medical University of Bialystok, Bialystok, Poland; [2]Department of Cardiology and Internal Diseases, Medical University of Bialystok, Bialystok, Poland

Correspondence: Diana A Dmuchowska, Department of Ophthalmology, Medical University of Bialystok, 15-276 Bialystok, 24a M.Sklodowskiej-Curie St, Bialystok, Poland, Tel +48857468372, Email diana.dmuchowska@umb.edu.pl

Purpose: Precapillary pulmonary hypertension (PPH) is associated with systemic microvascular remodeling, but the outer retina–choroid relationship remains poorly defined. The aim of this study was to evaluate macular retinal thickness and choroidal structure and to investigate the outer retina–choroid association in patients with catheter-confirmed PPH and healthy controls.

Methods: In this single-center cross-sectional study, 29 patients with PPH defined according to European Society of Cardiology criteria and 37 age- and sex-matched controls underwent enhanced depth imaging spectral-domain optical coherence tomography. Retinal layers were automatically segmented (with manual correction when needed). The Early Treatment Diabetic Retinopathy Study (ETDRS) grid was applied to define measurement subfields. Thickness and volume of the total retina, inner retina, outer nuclear layer (ONL), outer retinal layer (ORL), retinal pigment epithelium (RPE), and choroidal thickness were quantified. Binarized subfoveal scans were used to determine total, luminal, and stromal choroidal areas, and the macular choroidal vascularity index (mCVI). Group comparisons, correlation analyses, ROC curves, and univariate regression models were performed.

Results: Compared with controls, patients with PPH demonstrated reduced total macular thickness, ORL thickness, RPE thickness, and central macular choroidal thickness, whereas ONL thickness and mCVI did not differ significantly. In the PPH group, central macular ORL thickness was positively correlated with central macular choroidal thickness and negatively with mCVI (both $p \leq 0.006$). Central macular ORL thickness discriminated PPH from controls (AUC 0.818; sensitivity 85.7%; specificity 67.6%). In univariate regression analysis, ORL thickness was significantly associated with choroidal structural parameters ($p \leq 0.007$) and bosentan treatment ($p = 0.019$).

Conclusion: PPH is associated with thinning of the macular ORL, RPE, and choroid, accompanied by PPH-specific outer retina–choroid structural association absent in controls. ORL thickness may represent an adjunct structural indicator in PPH. These findings are exploratory and require validation in larger, longitudinal cohorts.

Keywords: choroid, retina, outer retinal layer, optical coherence tomography, choroidal vascularity index, bosentan

Introduction

Pulmonary hypertension (PH) is a hemodynamic disorder characterized by elevated mean pulmonary arterial pressure (mPAP). Precapillary PH (PPH) comprises forms in which pressure elevation originates in the pulmonary arterial bed, not the left heart. It is confirmed by right-heart catheterization.[1–6] Endothelial dysfunction, marked by increased production of vasoconstrictors such as endothelin and thromboxane and by reduced bioavailability of endogenous vasodilators including nitric oxide, prostacyclin, and natriuretic peptides, creates a persistent imbalance that favors vasoconstriction, platelet activation, and concentric remodeling of the pulmonary arterial wall, progressively raising pulmonary vascular resistance. If left untreated, PH leads to right ventricular failure.[2,5,7–10]

https://doi.org/10.2147/OPTH.S590272
Received: 19 December 2025
Accepted: 28 February 2026
Published: 19 March 2026

The inner retina is perfused by the central retinal artery, and the outer retina is supplied almost entirely by the choroid.[11,12] Given the exceptionally high metabolic activity of photoreceptors, a robust choroidal blood supply is indispensable to meet their oxygen and nutrient demands.[13] Enhanced depth imaging optical coherence tomography (EDI-OCT) enables noninvasive choroidal assessment.[14]

Two complementary metrics regarding the structural and vascular status of the choroid are used: choroidal thickness (CT) and the macular choroidal vascularity index (mCVI; calculated as the ratio of macular luminal area to macular total choroidal area). Because mCVI reflects the relative vascular component of the choroid rather than absolute thickness, it may provide additional structural information beyond CT.[11,15,16] In brief, PPH affects both the choroid and the retina, and the choroid in turn influences the outer retina. Both structures were evaluated in PH patients. Previous OCT and OCTA studies in PH have demonstrated alterations in retinal and choroidal vessel density, and choroidal thickness but the reported findings remain inconsistent.[4,17–22] Alterations in CT have also been linked to other cardiovascular and systemic conditions including carotid stenosis, systemic hypertension, arteriosclerosis, type 2 diabetes, and chronic heart failure with acute hypertension tending to increase CT, whereas chronic hypertension and heart failure are associated with CT reduction.[17–21]

Despite increasing evidence of retinal and choroidal involvement in PH, the structural association between the outer retina and the choroid has not been systematically investigated in patients with PH. This is the first study to address the link between the choroidal and outer retinal parameters in patients with PPH. The retina and pulmonary circulation share common features of microvascular networks susceptible to endothelial dysfunction and hypoxia-related remodeling. Anatomic, genetic, and functional parallels between the retinal and pulmonary microcirculations suggest that retinal imaging might offer a noninvasive window into pulmonary vascular remodeling in PH.[22] Structural alterations within the outer retina, which is dependent on choroidal perfusion, may therefore reflect systemic microvascular changes occurring in PPH.

Given the dependence of the outer retina on choroidal perfusion, we hypothesized that structural alterations in PPH would preferentially involve the outer retinal layer and demonstrate measurable associations with choroidal parameters. The aim of this study was to evaluate macular retinal and choroidal structure in patients with PPH and to investigate outer retina–choroid structural link.

Materials and Methods

This single-center cross-sectional study included 29 patients with PPH admitted for routine clinical assessment to the Department of Cardiology and Internal Diseases, at the Medical University of Bialystok, who were on stable pharmacotherapy, and 37 healthy controls. The study was conducted jointly by the Departments of Ophthalmology and Cardiology and Internal Diseases at the Medical University of Bialystok, Poland. The data were collected prospectively according to a predefined protocol. One eye per participant was randomly selected.

All participants underwent a comprehensive ophthalmic examination: refraction; best corrected distance visual acuity (BCDVA) measured on a Snellen chart and converted to logMAR; intraocular pressure (IOP) by dynamic contour tonometry (Pascal DCT; Ziemer Ophthalmic Systems, Port, Switzerland); keratometry and axial length (OA-2000; Tomey, Nagoya, Japan); autorefraction (KR-8900; Topcon, Tokyo, Japan); slit-lamp biomicroscopy; dilated fundus examination; and spectral-domain OCT with EDI mode (SD-OCT; Spectralis, Heidelberg Engineering, Heidelberg, Germany, 2016). Blood pressure was measured in the seated position after a 5-minute rest, immediately followed by OCT image acquisition.

Clinical and hemodynamic data were collected, including medical history, physical examination, right-heart catheterization, and echocardiography. Laboratory and functional assessments were performed (World Health Organization [WHO] functional class, presence of peripheral edema, N-terminal pro-B-type natriuretic peptide [NT-proBNP], and six-minute walk distance). We also recorded sex, current smoking status, duration of PPH, and medical therapy.

PPH was diagnosed according to European Society of Cardiology (ESC) guidelines, with right-heart catheterization confirming the precapillary profile. PPH was defined as mean pulmonary arterial pressure (mPAP) ≥ 25 mmHg, pulmonary arterial wedge pressure (PAWP) $\leq$ 15 mmHg, and pulmonary vascular resistance (PVR) $>$ 3 Wood units (WU).[5] Enrollment was performed in 2021–2022; therefore, classification followed the hemodynamic thresholds

recommended at that time. Given subsequent updates to the hemodynamic definition,[6] interpretation in cohorts defined by revised thresholds should be performed cautiously. The PPH cohort comprised idiopathic pulmonary arterial hypertension (PAH) and PPH associated with congenital heart disease or connective tissue disease, as well as chronic thromboembolic pulmonary hypertension (CTEPH). Participants with significant pulmonary parenchymal disease or pulmonary hypertension due to left-sided heart disease were excluded.[2,6] Echocardiographic characterization included tricuspid annular plane systolic excursion (TAPSE), right ventricular systolic function, tricuspid regurgitation peak gradient, estimated mean pulmonary arterial pressure (eMPAP), estimated pulmonary artery systolic pressure, right atrial pressure (RAP), right atrial area (RAA), and right ventricular diameter in the four-chamber (4CH) view.[6]

Inclusion criteria for both groups were age ≥ 18 years and written informed consent to participate in the study. Participants of the PPH group fulfilled the ESC criteria.[5] Controls were self-reported as healthy. Exclusion criteria for both groups were history of posterior segment surgery or intravitreal injections; cataract surgery performed less than 12 months before the examination; ocular or systemic disorders potentially affecting the choroid; prior retinal laser treatment; any fundus pathology or macular changes; and OCT scan quality < 25 dB. Participants with ametropia ≥ 3 diopters were excluded to reduce refractive error–related magnification effects that may influence lateral OCT measurements and choroidal area calculations.

The study adhered to the tenets of the Declaration of Helsinki and was approved by the Bioethics Committee of the Medical University of Bialystok (APK.002.290.2020). Written informed consent was obtained from all participants.

OCT Imaging and Analysis

All participants underwent SD-OCT, conducted by the same experienced examiner (AZ) under mydriasis at the same time of day, to minimize the influence of diurnal variations on choroidal thickness measurements. The images were independently evaluated by two investigators (AZ, BP). The macular SD-OCT imaging protocol included 25 raster scans (20° × 20°) and a single 30° linear EDI-OCT B-scan centered on the fovea. As outlined in our earlier publications,[23,24] the retinal layers were automatically delineated using Spectralis software within each ETDRS-defined subfield (version 6.7, Heidelberg Engineering, Heidelberg, Germany), including the internal limiting membrane (ILM), outer plexiform layer (OPL), external limiting membrane (ELM), retinal pigment epithelium (RPE), and Bruch's membrane (BM), while the choroidal–scleral junction (CSJ) was manually marked by adjusting the Bruch's membrane (BM) line to align with the CSJ. All automated segmentations were reviewed and manually corrected when necessary by experienced investigators to ensure anatomical accuracy.

The inner retina was defined as the region between the internal limiting membrane (ILM) and the outer boundary of the outer plexiform layer (OPL); the outer nuclear layer (ONL) as the region between the outer boundary of the OPL and the external limiting membrane (ELM); and the outer retinal layer (ORL) as the region extending from the ELM to Bruch's membrane (BM), as illustrated in Figure 1. The applied segmentation approach was based on both relevant literature[25] and the software integrated into the Spectralis device used for OCT imaging.

Mean retinal thickness and volume maps were automatically generated using the standardized Early Treatment Diabetic Retinopathy Study (ETDRS) grid.[26] We measured choroidal parameters by subtracting retinal parameters (area from the ILM to the BM) from the total area of the created map covering the region from the ILM to the manually marked choroidal–scleral junction). The present study primarily focused on the retinal thickness in 5 subfields: the central subfield (1-mm diameter) and the four inner ETDRS subfields within the 3-mm ring (inner superior, inner nasal, inner inferior, inner temporal), all centered on the fovea and the choroidal thickness values for the central 1 mm subfield. The central subfield was selected to correspond with the CVI assessment performed over a 1000 µm width and to ensure clarity in subsequent multiple comparisons (Supplementary Figure 1). In our study, we used the term "subfoveal" to specifically refer to the central point directly beneath the fovea (ie., a single-point measurement), whereas "central macular" referred to the 500 µm radius region centered on the fovea.

Binarization of Subfoveal Choroidal OCT B-Scans

Binarization of the macular choroid was performed by two independent researchers (AZ, BP) on a single horizontal 30° EDI-OCT B-scan centered on the fovea (500 µm nasally and temporally), averaged from 100 frames (Figure 2). Images

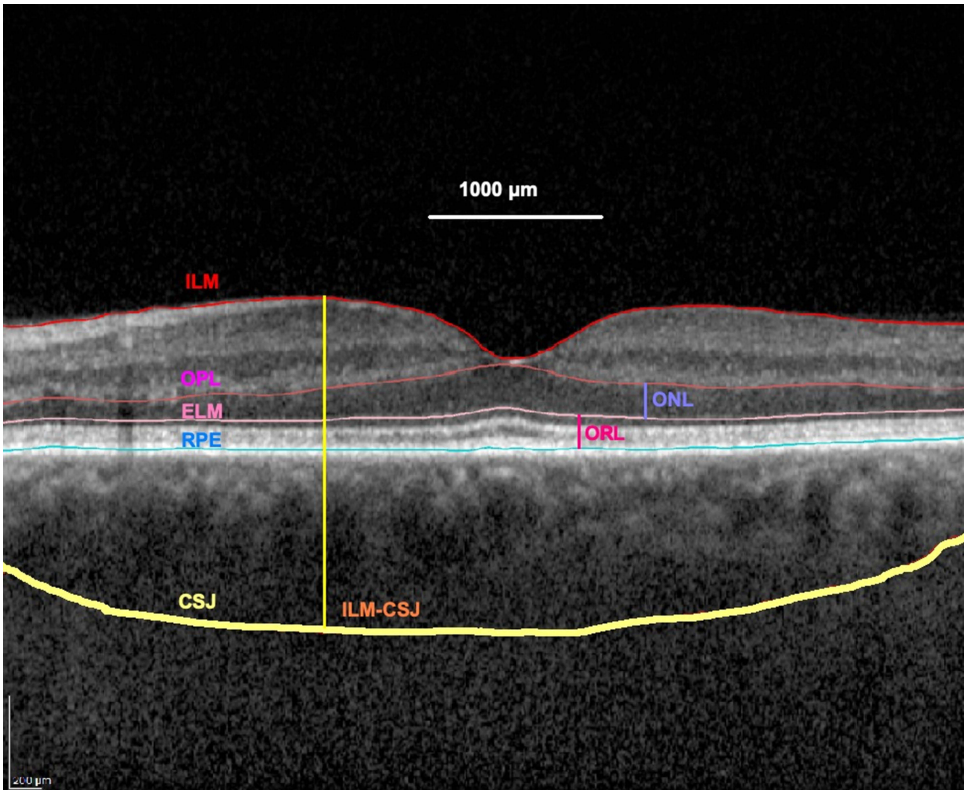

Figure 1 Retinal layer segmentation in the macula and choroidal-scleral junction (CSJ) marking.
Notes: The horizontal white line represents a width of 1000 µm. The scale bar is shown in the lower left corner. The color of each abbreviation corresponds to the color of the line representing the respective structure. The exception is ILM–CSJ, where the abbreviation is shown in orange and the corresponding measurement line in yellow for better visibility.
Abbreviations: CSJ, choroidal-scleral junction; ELM, external limiting membrane; ILM, internal limiting membrane; ILM-CSJ, distance from internal limiting membrane to choroidal–scleral junction; ONL, outer nuclear layer; OPL, outer plexiform layer; ORL, outer retinal layer; RPE, retinal pigment epithelium.

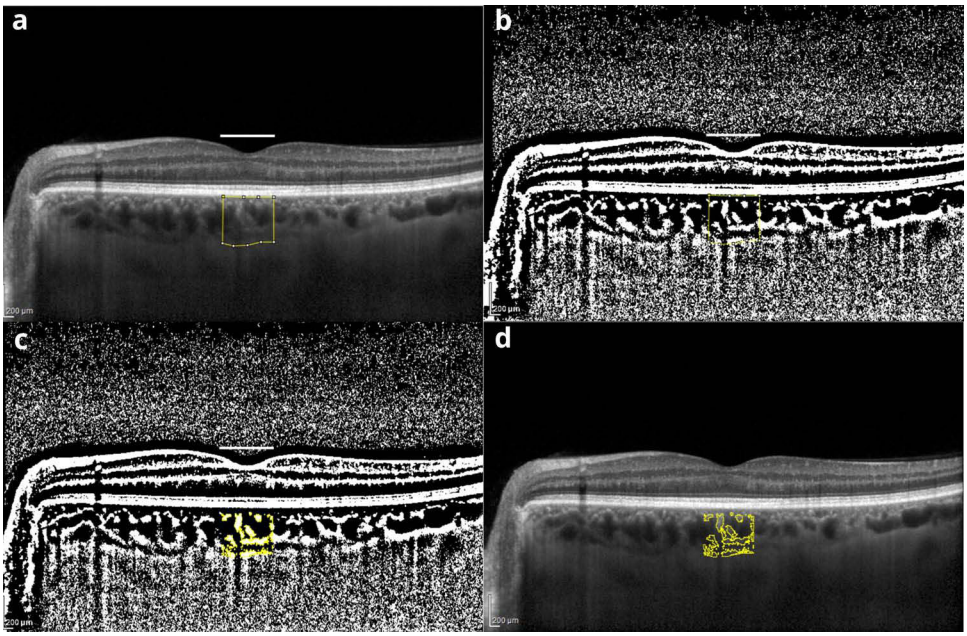

Figure 2 Choroidal image binarization workflow.
Notes: Macular total choroidal area (mTCA) was manually delineated from the outer border of Bruch's membrane to the choroidal–scleral junction using the polygon selection tool (**a**). Images were converted to 8-bit and binarized using the Niblack local adaptive thresholding algorithm (**b**). The binarized images were reconverted to RGB. Dark pixels corresponding to luminal areas were segmented with the Color Threshold tool (yellow outlines) (**c**) and the resulting luminal mask was overlaid on the original B-scan for verification (**d**). The binarization methodology has been described in detail previously.[20] The horizontal white line represents a width of 1000 µm. The scale bar is shown in the lower left corner.

were processed in ImageJ (NIH; https://imagej.nih.gov/ij) following the protocols of Sonoda et al and Agrawal et al[27–29] (Figures 2a–d).

The macular choroidal vascularity index (mCVI) was calculated as (mLA/mTCA) × 100%. The macular luminal area (mLA) and macular total choroidal area (mTCA) were measured, and the macular stromal area (mSA) was calculated as mTCA minus mLA. The parameters were assessed by two experienced researchers (AZ and BP) at the same time of the day in both groups, with the average of two measurements included in the analysis. Any doubts were resolved through discussion. Inter-rater measurement repeatability was evaluated using the intraclass correlation coefficient (ICC), and ICC values for mCVI, mTCA, and mLA exceeded 0.90, indicating high inter-rater reliability.

Statistical Analysis

The choroidal assessments by two investigators were averaged. Data are presented as n (% of group) for nominal variables or as mean ± SD or median (Q1; Q3) for continuous variables, as appropriate. Normality of distribution was assessed using Shapiro–Wilk test as well as skewness and kurtosis values. Group comparisons were performed using Fisher exact test or chi-square test for nominal data, Welch *t*-test or Mann–Whitney *U*-test for continuous data, as appropriate. Additionally, the MD (mean/median difference) between the two groups was calculated, including 95% confidence interval (CI). Benjamini–Hochberg correction for multiple comparisons was applied to control the false discovery rate at 5%, and both unadjusted and BH-adjusted p-values were reported. Benjamini–Hochberg adjustment was performed using the p.adjust function in R. Given the number of retinal and choroidal parameters evaluated, all analyses were considered exploratory, and p-values, particularly for secondary and post-hoc comparisons, should be interpreted with appropriate caution.

Predictive performance of the central macular retinal thickness for PPH vs. controls was compared using the area under the receiver operating characteristic (ROC) curve (AUC). Sensitivity and specificity values were reported at the cutoff points determined by the Youden index.

The univariate linear regression analysis was carried out to determine the association between ORL thickness and general/ophthalmological/cardiological parameters. For each linear regression model, the coefficient of determination (R^2) and adjusted coefficient of determination (adjusted R^2) were calculated and reported as measures of model fit.

The statistical analysis was conducted using R version 4.2.1 (R Foundation for Statistical Computing, Vienna, Austria). The post hoc power calculation was carried out by means of G*Power 3.1.9.7. software. All calculations were based on $\alpha = 0.05$.

Post-Hoc Power Calculation

The relatively small number of patients is due to the rarity of PPH and the sample size was partly determined by the number of participants who had met our inclusion criteria. The post-hoc power calculation, assuming $\alpha = 0.05$ and using the means and SDs obtained in the study for the comparison of PPH and control patients, resulted in the following power (1-β) values: total retinal thickness, central macular – 0.38; total retinal volume, central macular – 0.51; ORL thickness, central macular – 0.99; RPE thickness, central macular – 0.22; ONL thickness, central macular – 0.28; inner retinal thickness, central macular – 0.05; choroidal thickness, central macular – 0.96; mCVI – 0.16.

Results

Baseline Characteristics

The study cohort comprised 66 participants: 29 patients diagnosed with PPH and 37 healthy controls (Table 1). No statistically significant differences were observed between the groups regarding age, sex, smoking status, systolic blood pressure, AXL, IOP, BCDVA, keratometry, and spherical equivalent values ($p>0.05$ for all comparisons). Statistically significant differences were observed between the PPH and control groups in terms of diastolic blood pressure and consequently mean arterial pressure (MAP), both of which were lower in the PPH group ($p<0.05$). Additionally, caffeine consumption was significantly higher among individuals in the control group ($p=0.017$).

Table 1 Baseline Demographic, Clinical, and Ophthalmological Characteristics

Variable	Total	PPH Group	Control Group	p
Number of patients	66	29	37	
Age, (years)	52.62±12.64	55.38±15.40	50.46±9.65	0.140
Sex, n (%)				
Female	34 (51.5)	13 (44.8)	21 (56.8)	0.475
Male	32 (48.5)	16 (55.2)	16 (43.2)	
BP Systolic (mmHg)	122.58±17.41	118.41±11.87	126.48±20.78	0.069
BP Diastolic (mmHg)	77.53±10.64	73.41±9.24	81.39±10.55	**0.003**
MAP (mmHg)	92.55±11.31	88.41±8.75	96.42±12.17	**0.005**
Caffeine, n (%)	37 (56.1)	11 (37.9)	26 (70.3)	**0.017**
Nicotine (yes), n (%)	10 (15.2)	4 (13.8)	6 (16.2)	>0.999
AXL (mm)	23.45±1.09	23.60±1.19	23.33±1.01	0.345
logMAR, median (Q1;Q3)	0.00 (0.00;0.00)	0.00 (0.00;0.00)	0.00 (0.00;0.00)	0.250
IOP (mmHg)	15.49±2.89	15.51±3.76	15.47±2.01	0.964
SE (D)	0.22±1.33	0.12±1.11	0.30±1.50	0.590
K1 (D)	42.88±1.47	42.83±1.41	42.88±1.53	0.804
K2 (D)	43.77±1.53	43.83±1.42	43.72±1.64	0.725

Notes: Data are presented as mean±SD, unless otherwise indicated. Groups were compared with *t*-test or Mann–Whitney *U*-test for continuous variables and with chi-square test or Fisher exact test for nominal variables $p < 0.05$ in bold.

Abbreviations: AXL, axial length; BP, blood pressure; IOP, intraocular pressure; MAP, mean arterial pressure; PPH, precapillary pulmonary hypertension; Q1, quartile 1; Q3, quartile 3; K1, flat keratometry value; K2, steep keratometry value; SE, spherical equivalent.

The cardiac assessment of patients with PPH comprised medical history and physical examination, echocardiographic findings, right-heart catheterization, laboratory and functional test results, and details of current medical therapy and the underlying etiology of PPH (Table 2).

Table 2 Baseline Cardiological Clinical Characteristics of Patients with Precapillary Pulmonary Hypertension

Variable	Value
PPH duration (years), median (Q1;Q3)	5.00 (3.00;13.00)
NT-proBNP (pg/mL), median (Q1;Q3)	227.55 (155.93;992.33)
Presence of peripheral edema, n (%)	4 (13.8)
6MWT (m), mean±SD	437.38±146.82
Echocardiographic parameters	
TAPSE (mm), mean±SD	17.32±5.68
Tricuspid regurgitation peak gradient (mmHg), mean±SD	53.22±25.57

(*Continued*)

Table 2 (Continued).

Variable	Value
eMPAP (mmHg), mean±SD	39.04±16.00
RAP (mmHg), mean±SD	5.90±4.17
RAA(cm^2), median (Q1;Q3)	20.00 (17.00;27.00)
Right ventricle diameter in the 4CH view (cm), median (Q1;Q3)	4.60 (3.85;5.00)
Systolic pulmonary artery pressure (mmHg), mean±SD	52.36±26.71
Pharmacotherapy	
Sildenafil, yes, n (%)	16 (55.2)
Bosentan, yes, n (%)	11 (37.9)
Furosemid, yes, n (%)	11 (37.9)
PPH etiology	
Idiopathic, yes, n (%)	16 (55.2)
Congenital, n (%)	8 (27.6)
CTEPH, n (%)	3 (10.3)
Surgical defect, yes, n (%)	1 (3.4)
Non-surgical defect, yes, n (%)	2 (6.9)
Connective tissue diseases, n (%)	1 (3.4)

Notes: Q1, quartile 1; Q3, quartile. $p < 0.05$ in bold.
Abbreviations: CTEPH, chronic thromboembolic pulmonary hypertension; eMPAP, estimated mean pulmonary arterial pressure; NT-proBNP, N-terminal pro-B-type Natriuretic Peptide; PPH, precapillary pulmonary hypertension; RAA, right atrial area; RAP, right atrial pressure; TAPSE, Tricuspid Annular Plane Systolic Excursion; 4CH, four-chamber; 6MWT, six-minute walk test.

Between-Group Comparison of Retinal and Choroidal Parameters

Between-group comparison demonstrated that patients with PPH had significantly reduced total retinal thickness, ORL thickness, RPE thickness, and central macular choroidal thickness compared with controls across the majority of ETDRS subfields. The differences in the inner retinal thickness were less pronounced (Table 3, condensed). Complete ETDRS subfield data are provided in Supplementary Table 1 to improve clarity and readability of the main manuscript. In general, no differences in ONL thickness were found between PPH patients and controls.

Detailed choroidal thickness values in all ETDRS subfields were reported in our previous publication.[20]

No significant differences were observed in mTCA, mLA, mSA, or mCVI between the two groups ($p>0.05$), in contrast to the central macular choroidal thickness ($p<0.005$).

Intra-Group Correlations Between Outer Retinal and Choroidal Parameters

The correlations between choroidal parameters and outer retinal parameters were examined (Table 4). In the present study, the analysis focuses specifically on retina–choroid structural link and layer-specific associations. Consequently, only central macular choroidal thickness is presented for direct comparison. Several significant correlations were observed in the PPH group between the central macular ORL thickness and choroidal parameters ($p<0.05$). Additionally, a notable association was observed between the total central macular retinal thickness and the mCVI ($p=0.038$). No correlations between central macular thicknesses, namely total retinal, ONL, RPE, and other choroidal

https://doi.org/10.2147/OPTH.S590272

Table 3 (Condensed). Comparison of Retinal and Choroidal Parameters in Patients with Precapillary Pulmonary Hypertension and Controls

	Variable	p	B-H
Total Retinal Thickness [µm]	Outer T	0.180	0.200
	Inner T	**0.007**	**0.012**
	Central Macular	0.103	0.129
	Outer N	**0.001**[a]	**0.003**
	Inner N	**<0.001**[a]	**0.001**
	Outer S	**0.012**	**0.017**
	Inner S	**0.001**[a]	**0.003**
	Outer I	**0.006**	**0.012**
	Inner I	**<0.001**	**0.001**
	SFCT	0.442[a]	0.442
Total Retinal Volume [μm^3]	Outer T	0.237	0.237
	Inner T	**0.024**	**0.030**
	Central macular	0.079	0.088
	Outer N	**<0.001**	**0.001**
	Inner N	**0.001**	**0.003**
	Outer S	**0.012**	**0.017**
	Inner S	**0.001**	**0.003**
	Outer I	**0.005**	**0.008**
	Inner I	**<0.001**	**0.001**
	Total	**0.002**	**0.004**
ORL Thickness [µm]	Inner T	**0.001**	**0.001**
	Central Macular	**<0.001**	**<0.001**
	Inner N	**0.001**	**0.001**
	Inner S	**<0.001**	**<0.001**
	Inner I	**0.031**	**0.031**
RPE Thickness [µm]	Inner T	**0.021**	**0.026**
	Central Macular	0.234	0.234
	Inner N	**0.013**	**0.022**
	Inner S	**<0.001**	**0.001**
	Inner I	**0.001**	**0.003**

(*Continued*)

Table 3 (Continued).

	Variable	p	B-H
ONL Thickness [µm]	Inner T	0.387	0.484
	Central Macular	0.173	0.387
	Inner N	0.575	0.575
	Inner S	0.232	0.387
	Inner I	0.175	0.387
Inner Retinal Thickness [µm]	Inner T	0.054	0.086
	Central Macular	0.839	0.839
	Inner N	**<0.001**[a]	**<0.001**
	Inner S	0.069[a]	0.086
	Inner I	**0.012**	**0.030**
Choroidal Parameters	Central Macular Choroidal Thickness [µm]	**0.001**	**0.003**
	mTCA [μm^2]	0.120	0.240
	mLA [μm^2]	0.084	0.240
	mSA [μm^2]	0.229	0.305
	mCVI [%]	0.349	0.349

Notes: Groups were compared through the *t*-test or Mann–Whitney U test[a]. Benjamini–Hochberg (BH) correction for multiple comparisons was applied separately to each group of parameters as per first column, i.e. retinal thickness parameters (10 comparisons), retinal volume parameters (10 comparisons), ORL thickness parameters (5 comparisons) etc. The conventional ETDRS grid with nine subfields: a central macular field (central field within a 500-µm radius), four inner subfields (within a 500–1500-µm radius) and four outer subfields (within a 1500–3000-µm radius). A central macular and four inner subfields presented for clarity. $p<0.05$ in bold.

Abbreviations: I, inferior; mCVI, macular choroidal vascularity index; mLA, macular luminal area; mSA, macular stromal area; mTCA, macular total choroidal area; N, nasal; ONL, outer nuclear layer; ORL, outer retinal layer; RPE, retinal pigment epithelium; S, superior; SFCT, subfoveal choroidal thickness; T, temporal.

Table 4 Correlations Between Outer Retinal and Choroidal Parameters in Patients with Precapillary Pulmonary Hypertension and Controls

Retinal Parameters	Choroidal Parameters	PPH Group		Control Group	
		rho	p	rho	p
ORL Thickness Central Macular [µm]	Choroidal Thickness Central Macular [µm]	0.50	**0.006**	−0.20	0.231
	mTCA [μm^2]	0.56	**0.004**	−0.16	0.351
	mLA [μm^2]	0.53	**0.007**	−0.16	0.329
	mSA [μm^2]	0.59	**0.002**	−0.14	0.419
	mCVI [%]	−0.55	**0.005**	−0.0002	0.999

(*Continued*)

https://doi.org/10.2147/OPTH.S590272

Table 4 (Continued).

Retinal Parameters	Choroidal Parameters	PPH Group		Control Group	
		rho	p	rho	p
RPE Thickness Central Macular [µm]	Choroidal Thickness Central Macular [µm]	0.01	0.944	0.07	0.683
	mTCA [μm^2]	0.30	0.144	0.09	0.599
	mLA [μm^2]	0.29	0.156	0.05	0.755
	mSA [μm^2]	0.31	0.137	0.14	0.394
	mCVI [%]	−0.27	0.207	−0.25	0.134
ONL Thickness Central Macular [µm]	Choroidal Thickness Central Macular [µm]	−0.06	0.766	0.12	0.490
	mTCA [μm^2]	0.16	0.444	0.04	0.799
	mLA [μm^2]	0.17	0.424	0.07	0.674
	mSA [μm^2]	0.14	0.493	−0.01	0.969
	mCVI [%]	0.04	0.866	0.09	0.589
Total Retinal Thickness Central Macular [µm]	Choroidal Thickness Central Macular [µm]	−0.14	0.464	0.01	0.959
	mTCA [μm^2]	0.13	0.543	−0.11	0.510
	mLA [μm^2]	0.10	0.643	−0.14	0.400
	mSA [μm^2]	0.18	0.401	−0.05	0.749
	mCVI [%]	−0.43	**0.038**	−0.23	0.170

Notes: p<0.05 in bold. For clarity, the correlations of the parameters from the central ETDRS subfield were included.
Abbreviations: mCVI, macular choroidal vascularity index; mLA, macular luminal area; mSA, macular stromal area; mTCA, macular total choroidal area; ONL, outer nuclear layer; ORL, outer retinal layer; rho, Spearman correlation coefficient; RPE, retinal pigment epithelium.

parameters were found. No significant correlations between outer retinal and choroidal parameters were observed in the control group (p>0.05).

Cut-off Point Calculation for Central Macular Retinal Thickness Parameters

Receiver Operating Characteristic (ROC) curves (Figure 3) were generated to determine the optimal cut-off points for retinal parameters that demonstrated statistically significant between-group differences to discriminate between PPH patients and control subjects. The cut-off point calculation was based on Youden's index. The sensitivity, specificity, accuracy, negative predictive value (NPV) and positive predictive value (PPV) of the cut-off points were calculated as well. Table 5 presents ROC performance for central macular ORL thickness and central macular total retinal thickness. Central macular ORL thickness was defined as the distance between the ELM and BM within the ETDRS central subfield. It showed the most consistent correlations with choroidal structural parameters in the PPH group and demonstrated high post-hoc statistical power compared with other retinal metrics. Central macular total retinal thickness, which proved to correlate with mCVI, is presented for comparison. Given the exploratory design and sample size, ROC performance estimates should be interpreted as preliminary. The ROC performance of selected choroidal parameters has been reported previously.[21]

Intra-Group Univariate Regressions to Identify Factors Related to the Thickness of Outer Retinal Layer (ORL)

We additionally aimed to identify factors associated with the central macular ORL thickness in patients with PPH and controls. In addition to ophthalmological parameters, univariate regression analyses incorporated a range of clinical, as

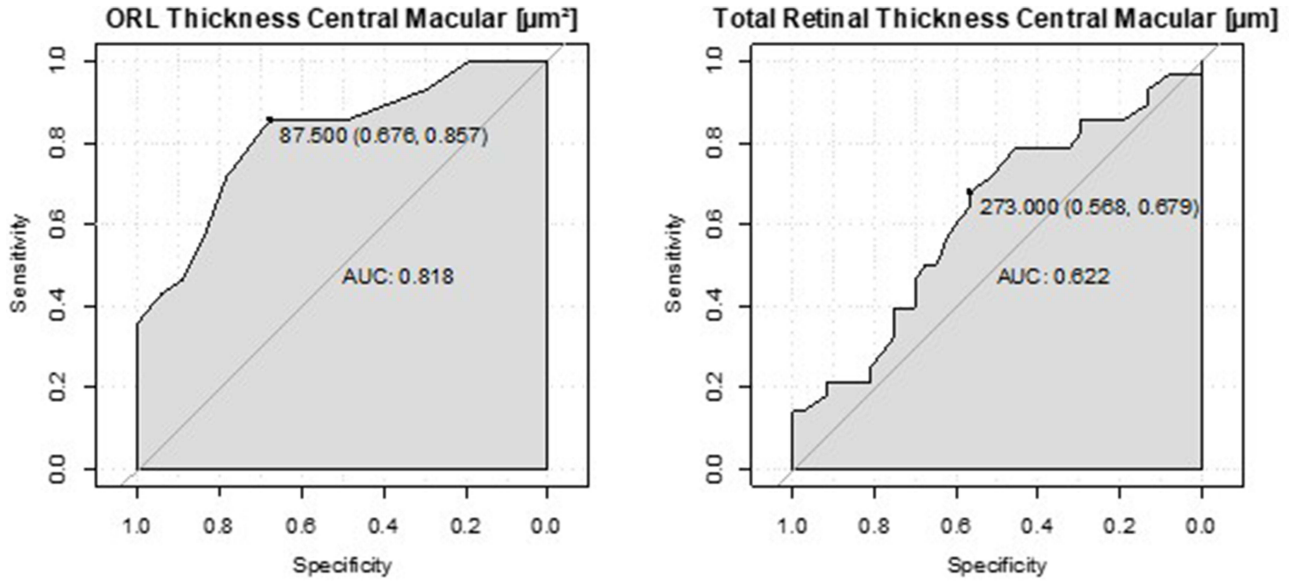

Figure 3 Receiver operating characteristic (ROC) curves of selected central macular retinal parameters discriminating precapillary pulmonary hypertension from controls. **Abbreviations**: AUC, area under the curve; ORL, outer retinal layer; PPH, precapillary pulmonary hypertension.

well as cardiological factors, including current pharmacotherapy. Several statistically significant associations were identified between central macular ORL thickness and various parameters in the PPH group (Table 6). ORL thickness was found to be associated with choroidal parameters, including mCVI, mTCA, mLA, mSA, central macular choroidal thickness, central macular choroidal volume, and total choroidal volume ($p<0.005$ for all). Additionally, a significant association was observed between ORL thickness and the use of bosentan ($p=0.019$).

Table 5 Performance of Selected Retinal Parameters in the Prediction of Precapillary Pulmonary Hypertension

	PPH vs. Controls						
	Optimal cut-off point	**AUC (95% CI)**	**Sensitivity (%)**	**Specificity (%)**	**Accuracy (%)**	**PPV (%)**	**NPV (%)**
ORL Thickness Central Macular [µm]	87.50	0.818 (0.713; 0.922)	85.7	67.6	75.4	66.7	86.2
Total Retinal Thickness Central Macular [µm]	273.00	0.622 (0.482; 0.762)	67.9	56.8	61.5	54.3	70.0

Abbreviations: AUC, area under the curve; ORL, outer retinal layer; PPH, precapillary pulmonary hypertension; PPV, positive predictive value; NPV, negative predictive value.

Table 6 Univariate Linear Regression Analysis of Factors Associated with ORL Thickness in Patients with Precapillary Pulmonary Hypertension

	Independent Variable:	**β**	**SE (Standard Error)**	**B**	**p**	**R2**	**Adjusted R2**
ORL Thickness Central Macular [µm]	General parameters						
	Age [years]	−0.044	0.043	−0.194	0.315	0.039	0.002
	Sex, male	0.036	1.360	–	0.979	0.001	−0.038
	MAP [mmHg]	−0.134	0.075	−0.332	0.080	0.113	0.079
	Caffeine, yes	0.544	1.412	–	0.703	0.006	−0.033
	Nicotine, yes	−2.520	2.138	–	0.249	0.051	0.014

(*Continued*)

https://doi.org/10.2147/OPTH.S590272

Table 6 (Continued).

	Independent Variable:	β	SE (Standard Error)	B	p	R2	Adjusted R2
	Ophthalmological parameters						
	IOP [mmHg]	−0.248	0.242	−0.197	0.315	0.039	0.002
	AXL [mm]	0.092	0.581	0.031	0.875	0.001	−0.037
	Retinal Volume Total [μm^3]	−1.695	1.543	−0.211	0.282	0.044	0.008
	Choroidal Thickness Central Macular [μm]	0.017	0.006	0.504	**0.006**	0.254	0.226
	SFCT [μm]	0.014	0.006	0.422	**0.025**	0.178	0.147
	Choroidal Volume Central Macular [mm^3]	20.989	7.154	0.499	**0.007**	0.249	0.219
	Choroidal Volume Total [mm^3]	0.886	0.236	0.593	**0.001**	0.351	0.326
	mCVI [%]	−0.795	0.257	−0.516	**0.005**	0.303	0.271
	mTCA [μm^2]	0.000	0.000	0.518	**0.004**	0.310	0.280
	mLA [μm^2]	0.000	0.000	0.492	**0.007**	0.279	0.248
	mSA [μm^2]	0.000	0.000	0.548	**0.002**	0.347	0.319
	Cardiological parameters						
	PPH duration, [years]	0.043	0.107	0.093	0.692	0.008	−0.040
	WHO functional class [1–4]	1.343	1.268	0.216	0.300	0.045	0.005
	NT-proBNP [pg/mL]	−0.001	0.002	−0.083	0.706	0.007	−0.040
	Presence of peripheral edema, yes	−0.100	1.868	-	0.958	0.000	−0.045
	6MWT [m]	0.001	0.005	0.042	0.842	0.002	−0.042
	TAPSE [mm]	−0.001	0.137	−0.002	0.995	0.000	−0.043
	Tricuspid regurgitation peak gradient [mmHg]	−0.007	0.032	−0.050	0.832	0.002	−0.048
	eMPAP [mmHg]	−0.013	0.049	−0.058	0.799	0.003	−0.044
	RAP [mmHg]	−0.274	0.207	−0.324	0.203	0.089	0.038
	RAA [cm^2]	−0.219	0.124	−0.344	0.089	0.131	0.089
	Right ventricle 4CH view [cm]	−1.531	0.845	−0.352	0.083	0.120	0.084
	Systolic pulmonary artery pressure [mmHg]	−0.023	0.031	−0.173	0.476	0.027	−0.024
	Sildenafil, yes	2.000	1.417	-	0.171	0.077	0.038
	Bosentan, yes	3.199	1.271	-	**0.019**	0.216	0.182
	Furosemid, yes	−2.369	1.352	-	0.092	0.109	0.074
	Idiopathic, yes	1.705	1.228	-	0.177	0.072	0.034

Notes: $p < 0.05$ in bold.

Abbreviations: 4CH, four-chamber; 6MWT, six-minute walk test; AXL, axial length; B, unstandardized beta coefficient; eMPAP, estimated mean pulmonary arterial pressure; IOP, intraocular pressure; MAP, mean arterial pressure; mCVI, macular choroidal vascularity index; mLA, macular luminal area; mSA, macular stromal area; mTCA, macular total choroidal area; NT-proBNP, N-terminal pro-B-type natriuretic peptide; PPH, precapillary pulmonary hypertension; RAA, right atrial area; RAP, right atrial pressure; SFCT, subfoveal choroidal thickness; TAPSE, tricuspid annular plane systolic excursion; β, standardized beta coefficient.

No associations were identified in the control group. (Supplementary Table 2).

Discussion

In this study, patients with PPH had reduced macular retinal thickness and volume, ORL thickness, RPE thickness, and central macular choroidal thickness, whereas ONL thickness, and mCVI were comparable. In PPH, central macular ORL thickness correlated with choroidal metrics, suggesting a structural relationship between outer retinal thickness and choroidal parameters. The changes within ORL are of particular interest as it contains photoreceptors, which are among the most metabolically active cells in the retina. Even minor impairments in choroidal perfusion or dysfunction of the RPE can translate into structural damage in the ORL and potentially compromise photoreceptor function, thereby directly affecting visual function.[30] Nonetheless, the magnitude of the observed differences in layer thickness was relatively small in absolute terms and binocular visual acuity remained normal in both groups. The findings therefore reflect subtle structural alterations rather than clinically overt retinal dysfunction, and their prognostic and functional relevance in PPH remains to be elucidated.

Notably, post-hoc power was high for central macular ORL thickness and choroidal thickness, but low for several other retinal layer parameters, suggesting that some true differences may have remained undetected. Given the metabolic dependence of the outer retina on choroidal perfusion, the observed associations between ORL thickness and choroidal parameters suggest the structural association within this complex in PPH.[11,12,31]

Previous OCT and OCTA studies have demonstrated retinal microvascular rarefaction and altered choroidal thickness in pulmonary hypertension. Albeit, findings remain heterogeneous and the relationship between outer retinal structure and choroidal metrics has not been previously examined in precapillary disease. In the majority of available studies concerning PPH, choroidal thickness was assessed, along with evaluations of the superficial and deep vascular plexuses using OCTA.

DuPont et al demonstrated higher retinal vascular tortuosity in PAH versus controls; retinal vascular parameters correlated with disease severity, and changes may track pulmonary vascular disease progression.[32] A recent expert review on extrapulmonary manifestations of PAH likewise highlights ocular involvement including retinal microvascular alterations and choroidal changes and underscores OCT/OCTA as accessible tools to capture systemic microvascular remodeling beyond the lung. It also positions ophthalmic metrics as candidate biomarkers for longitudinal monitoring.[33] In our previous study we demonstrated that patients with PPH had a markedly decreased choroidal thickness and volume compared to controls.[21] PAH/PPH can affect the microvasculature of the retina and optic nerve. OCTA has detected microvascular rarefaction, and OCT has demonstrated structural changes. Prior reports show reduced macular[4,34–37] and peripapillary vessel density with thinning of retinal nerve fiber layer (RNFL) and ganglion cell complex (GCC).[35] Choroidal results are inconsistent with some studies noting increased subfoveal CT[35] and others reduced subfoveal CT[4,21] These discrepancies may reflect differences in disease phenotype, hemodynamic profile, and chronicity. Choroidal thinning in our cohort may reflect chronic microvascular remodeling due hypoxia- and endothelial damage rather than acute hemodynamic congestion. The relatively long median disease duration supports a chronic remodeling mechanism. Longitudinal studies are required to confirm this hypothesis.

There is a lack of studies focusing on the inner retinal layers and directly examining the relationship between the choroid and the retina, which limits our ability to make direct comparisons.

Univariate regression analysis was subsequently employed to evaluate the associations between ORL thickness and selected ocular parameters, cardiovascular parameters, and pharmacological treatment variables in both PPH patients and control subjects. The thickness of the ORL was associated with all evaluated choroidal parameters, and with both central macular and total choroidal volume.

The impact of pharmacological therapy in patients with PPH should not be overlooked. Targeted therapies are established primarily for PAH (WHO Group 1); in other forms of PPH, disease-specific treatment is limited and remains indication-dependent. In PAH, therapies act mainly through the endothelin, nitric oxide– cyclic guanosine monophosphate, and prostacyclin pathways, including endothelin-receptor antagonists (eg., bosentan), phosphodiesterase-5 inhibitors (eg., sildenafil), and prostacyclin analogues. In other PPH groups, management generally focuses on treatment of the underlying condition, anticoagulation when indicated (notably in CTEPH), and supportive care, including diuretics

such as furosemide to control congestion.[38] Our study included 16 patients receiving sildenafil (daily dose: 2×25 mg to 3×40 mg) and 11 patients treated with bosentan (2×125 mg daily). In the univariate regression analysis, ORL thickness was significantly associated with bosentan use, explaining approximately 20% of its variance. Currently, there is a lack of evidence from the literature directly evaluating the impact of bosentan on human retinal morphology. Given the small and clinically heterogeneous cohort, this observation should be interpreted as exploratory and hypothesis-generating. No significant association was observed between sildenafil use and retinal or choroidal parameters, which may reflect chronic dosing, and sample size limitations. This is not in accordance with the data from the literature, where the impact of sildenafil use on CT is reported. Several factors may account for this discrepancy. Experimental and clinical studies evaluating sildenafil have often used higher single doses (100–200 mg) in otherwise healthy volunteers or in patient populations with different systemic profiles than those with PPH, and have primarily focused on short-term hemodynamic or choroidal effects.[39] Taken together, our findings may suggest a more pronounced structural impact of bosentan on the outer retina–choroid complex in PPH, although this hypothesis requires confirmation in larger, longitudinal studies.

The present study is not without limitations. First, this was a single-center study including a relatively small number of patients with PPH, which reflects the low prevalence of the disease, but limits statistical power and generalizability. The inclusion of 29 patients with a confirmed diagnosis of PPH aligns with the cohort sizes reported in comparable studies.[4,35] Second, the PPH cohort was clinically heterogeneous and comprised idiopathic PAH, PPH associated with congenital heart disease or connective tissue disease, and CTEPH. Due to limited subgroup sizes, phenotype-specific analyses were not feasible. Therefore, the results represent aggregated effects across different PPH entities. Third, the cross-sectional design precludes causal inference and does not allow assessment of temporal changes in retinal and choroidal structure or their relationship to treatment response and clinical outcomes. Fourth, multivariable modeling was not performed due to sample size constraints. Therefore, the observed associations may be influenced by residual confounding and should be interpreted cautiously. Finally, although we applied the Benjamini–Hochberg procedure to control the false discovery rate, we performed a number of statistical comparisons across multiple retinal and choroidal parameters. The analyses should therefore be regarded as exploratory.

Strengths of this study include a well-phenotyped, catheter-confirmed PPH cohort defined according to ESC criteria. All participants underwent comprehensive cardiological and ophthalmological assessment, allowing meaningful integration of retinal and choroidal metrics with systemic disease characteristics and targeted therapy. EDI-OCT was acquired by a single experienced examiner within a fixed morning time window to minimise diurnal variability in choroidal thickness. Detailed layer-specific macular analysis and quantitative choroidal binarization were performed, showing excellent inter-observer reproducibility. To our knowledge, this is the first study to characterize the structural associations between the macular outer retina and choroidal structure in PPH and to relate these metrics to cardiological parameters and specific PPH therapies.

Future directions should include larger, multicenter, and longitudinal studies to determine whether outer retinal and choroidal metrics predict disease progression, clinical outcomes, and response to targeted PPH therapies. Incorporating OCTA and other functional imaging could clarify how structural changes relate to microvascular perfusion. Data on swept-source OCT (SS-OCT) in PPH remain limited to case reports. Owing to its longer wavelength and improved penetration SS-OCT may enable more reliable delineation of the CSJ and more accurate volumetric assessment of choroidal remodeling than SD-OCT. These approaches may help refine the interpretation of choroidal changes observed in PPH. The clinical significance of reduced ORL thickness remains to be determined.

In summary, PPH is associated with thinning of the macular ORL and RPE and with reduced central macular choroidal thickness, while overall choroidal structure appears largely preserved. The selective structural link between outer retinal and choroidal metrics in PPH and the good discriminative performance of central macular ORL thickness support the use of OCT-derived outer retinal measures as promising candidate research indicators of microvascular involvement in this condition. At present, these OCT-derived metrics should be viewed as research tools rather than established clinical biomarkers, and further work is needed to define thresholds, assess reproducibility across devices and centers, characterize longitudinal trajectories, and determine their incremental value over standard cardiological assessment.

AI Statement

Generative AI (ChatGPT, version 5.2, OpenAI; https://openai.com) was used solely for language editing and stylistic refinement of the manuscript on December 17, 2025, without contributing to scientific content or interpretation; the authors take full responsibility for the accuracy, originality, and integrity of the text, including verification of references and ensuring absence of plagiarism.

Data Sharing Statement

Anonymized data supporting the findings of this study and analysis scripts used for statistical evaluation are available from the corresponding author upon reasonable request. Image processing and binarization procedures were performed using standardized workflows to facilitate reproducibility.

Funding

This work was supported by the Medical University of Bialystok, Poland (grant no B.SUB.23.526 to Diana Anna Dmuchowska).

Disclosure

Professor Karol Kaminski reports personal fees from MSD, Janssen, and AOP, outside the submitted work. The authors declare no other conflicts of interest in this work.

References

1. Simonneau G, Hoeper MM. The revised definition of pulmonary hypertension: exploring the impact on patient management. *Eur Heart J Suppl*. 2019;21(Suppl K):K4–K8. doi:10.1093/eurheartj/suz211
2. Bousseau S, Sobrano Fais R, Gu S, Frump A, Lahm T. Pathophysiology and new advances in pulmonary hypertension. *BMJ Med*. 2023;2(1): e000137. doi:10.1136/bmjmed-2022-000137
3. Gelzinis TA. Pulmonary hypertension in 2021: part i-definition, classification, pathophysiology, and presentation. *J Cardiothorac Vasc Anesth*. 2022;36(6):1552–1564. doi:10.1053/j.jvca.2021.06.036
4. Krajewski P, Turczyńska M, Gołębiewska J, Roik M, Brydak-Godowska J. Optical coherence tomography angiography findings in patients with chronic thromboembolic pulmonary hypertension. *Retina*. 2022;42(12):2354–2360. doi:10.1097/IAE.0000000000003607
5. Humbert M, Guignabert C, Bonnet S, et al. Pathology and pathobiology of pulmonary hypertension: state of the art and research perspectives. *Eur Respir J*. 2019;53(1):1801887. doi:10.1183/13993003.01887-2018
6. Humbert M, Kovacs G, Hoeper MM, et al. [2022 ESC/ERS Guidelines for the diagnosis and treatment of pulmonary hypertension]. *G Ital Cardiol*. 2023;24(4 Suppl 1):e1–e116. doi:10.1714/4014.39906
7. Spieker LE, Noll G, Ruschitzka FT, Maier W, Lüscher TF. Working under pressure: the vascular endothelium in arterial hypertension. *J Hum Hypertens*. 2000;14(10–11):617–630. doi:10.1038/sj.jhh.1001012
8. Szulcek R, Happé CM, Rol N, et al. Delayed microvascular shear adaptation in pulmonary arterial hypertension. role of platelet endothelial cell adhesion molecule-1 cleavage. *Am J Respir Crit Care Med*. 2016;193(12):1410–1420. doi:10.1164/rccm.201506-1231OC
9. Hoeper MM, Meyer K, Rademacher J, Fuge J, Welte T, Olsson KM. Diffusion capacity and mortality in patients with pulmonary hypertension due to heart failure with preserved ejection fraction. *JACC Heart Fail*. 2016;4(6):441–449. doi:10.1016/j.jchf.2015.12.016
10. Tuder RM, Archer SL, Dorfmüller P, et al. Relevant issues in the pathology and pathobiology of pulmonary hypertension. *J Am Coll Cardiol*. 2013;62(25 Suppl):D4–12. doi:10.1016/j.jacc.2013.10.025
11. Pournaras CJ, Rungger-Brändle E, Riva CE, Hardarson SH, Stefansson E. Regulation of retinal blood flow in health and disease. *Prog Retin Eye Res*. 2008;27(3):284–330. doi:10.1016/j.preteyeres.2008.02.002
12. Böhm EW, Pfeiffer N, Wagner FM, Gericke A. Methods to measure blood flow and vascular reactivity in the retina. *Front Med*. 2022;9:1069449. doi:10.3389/fmed.2022.1069449
13. Agrawal R, Ding J, Sen P, et al. Exploring choroidal angioarchitecture in health and disease using choroidal vascularity index. *Prog Retin Eye Res*. 2020;77:100829. doi:10.1016/j.preteyeres.2020.100829
14. Spaide RF, Koizumi H, Pozzoni MC. Enhanced depth imaging spectral-domain optical coherence tomography. *Am J Ophthalmol*. 2008;146 (4):496–500. doi:10.1016/j.ajo.2008.05.032
15. Singh SR, Vupparaboina KK, Goud A, Dansingani KK, Chhablani J. Choroidal imaging biomarkers. *Surv Ophthalmol*. 2019;64(3):312–333. doi:10.1016/j.survophthal.2018.11.002
16. Usui S, Ikuno Y, Akiba M, et al. Circadian changes in subfoveal choroidal thickness and the relationship with circulatory factors in healthy subjects. *Invest Ophthalmol Vis Sci*. 2012;53(4):2300–2307. doi:10.1167/iovs.11-8383
17. Yeung SC, You Y, Howe KL, Yan P. Choroidal thickness in patients with cardiovascular disease: a review. *Surv Ophthalmol*. 2020;65(4):473–486. doi:10.1016/j.survophthal.2019.12.007
18. Kim M, Kim RY, Kim JY, Park YH. Correlation of systemic arterial stiffness with changes in retinal and choroidal microvasculature in type 2 diabetes. *Sci Rep*. 2019;9(1):1401. doi:10.1038/s41598-018-37969-7
19. Wang H, Wang YL, Li HY. Subfoveal choroidal thickness and volume in severe internal carotid artery stenosis patients. *Int J Ophthalmol*. 2017;10 (12):1870–1876. doi:10.18240/ijo.2017.12.13

20. Pieklarz B, Gińdzieńska-Sieśkiewicz E, Zawadzka I, et al. Macular choroidal thickness, volume, and vascularity index in patients with systemic sclerosis. *Graefes Arch Clin Exp Ophthalmol*. 2023;262:1475–1487. doi:10.1007/s00417-023-06342-4
21. Zonenberg A, Ptaszyńska K, Szwedowicz A, et al. Linking cardiological parameters and choroidal changes in patients with precapillary pulmonary hypertension: a cross-sectional study. *Sci Rep*. 2025;15(1):31693. doi:10.1038/s41598-025-17425-z
22. Nickel NP, Shamskhou EA, Razeen MA, et al. Anatomic, genetic and functional properties of the retinal circulation in pulmonary hypertension. *Pulm Circ*. 2020;10(2):2045894020905508. doi:10.1177/2045894020905508
23. Sidorczuk P, Obuchowska I, Konopinska J, Dmuchowska DA. Correlation between choroidal vascularity index and outer retina in patients with diabetic retinopathy. *J Clin Med*. 2022;11(13). doi:10.3390/jcm11133882
24. Leoniuk A, Pieklarz B, Gińdzieńska-Sieśkiewicz E, et al. Is there a link between choroidal and retinal parameters in patients with systemic sclerosis? A prospective study. *Photodiagnosis Photodyn Ther*. 2025;53:104568. doi:10.1016/j.pdpdt.2025.104568
25. Ehnes A, Wenner Y, Friedburg C, et al. Optical Coherence Tomography (OCT) device independent intraretinal layer segmentation. *Transl Vis Sci Technol*. 2014;3(1):1. doi:10.1167/tvst.3.1.1
26. Grading diabetic retinopathy from stereoscopic color fundus photographs--an extension of the modified Airlie House classification. ETDRS report number 10. early treatment diabetic retinopathy study research group. *Ophthalmology*. 1991;98(5 Suppl):786–806. doi:10.1016/S0161-6420(13)38012-9
27. Sonoda S, Sakamoto T, Yamashita T, et al. Luminal and stromal areas of choroid determined by binarization method of optical coherence tomographic images. *Am J Ophthalmol*. 2015;159(6):1123–1131.e1. doi:10.1016/j.ajo.2015.03.005
28. Agrawal R. Optical coherence tomography: a potential noninvasive follow-up tool in multiple sclerosis. *Invest Ophthalmol Vis Sci*. 2016;57(4):2318. doi:10.1167/iovs.16-19605
29. Agrawal R, Li LK, Nakhate V, Khandelwal N, Mahendradas P. Choroidal vascularity index in vogt-koyanagi-harada disease: an EDI-OCT derived tool for monitoring disease progression. *Transl Vis Sci Technol*. 2016;5(4):7. doi:10.1167/tvst.5.4.7
30. Kurihara T, Westenskow PD, Gantner ML, et al. Hypoxia-induced metabolic stress in retinal pigment epithelial cells is sufficient to induce photoreceptor degeneration. *Elife*. 2016;5. doi:10.7554/eLife.14319
31. Bill A. Blood circulation and fluid dynamics in the eye. *Physiol Rev*. 1975;55(3):383–417. doi:10.1152/physrev.1975.55.3.383
32. DuPont M, Lambert S, Rodriguez-Martin A, et al. Retinal vessel changes in pulmonary arterial hypertension. *Pulm Circ*. 2022;12(1):e12035. doi:10.1002/pul2.12035
33. Singh N, Al-Naamani N, Brown MB, et al. Extrapulmonary manifestations of pulmonary arterial hypertension. *Expert Rev Respir Med*. 2024;18(3–4):189–205. doi:10.1080/17476348.2024.2361037
34. Lewczuk N, Zdebik A, Bogusławska J, Turno-Kręcicka A, Misiuk-Hojło M. Ocular manifestations of pulmonary hypertension. *Surv Ophthalmol*. 2019;64(5):694–699. doi:10.1016/j.survophthal.2019.02.009
35. Gu S, Li Z, Zhang Y, et al. Optical coherence tomography angiography findings of microvascular and neural changes in primary pulmonary hypertension. *Retina*. 2021;41(4):784–792. doi:10.1097/IAE.0000000000002940
36. Hekimsoy V, Kılınç Hekimsoy H, Şekeroğlu MA, Kaya EB, Tokgözoğlu L. The relationship between retinal microcirculation and right heart catheterization and echocardiography findings in patients with idiopathic pulmonary arterial hypertension. *Microcirculation*. 2021;28(6):e12704. doi:10.1111/micc.12704
37. Catarina F, Catarina CF, Ricardo MS, et al. Optical coherence tomography angiography in pulmonary hypertension. presented at: Euretina. Available from: https://euretina.org/resource/abstract_2021_optical-coherence-tomography-angiography-in-pulmonary-hypertension/. Accessed September 10, 2021.
38. Galiè N, Humbert M, Vachiery J-L. "2015 ESC/ERS Guidelines for the diagnosis and treatment of pulmonary hypertension. The joint task force for the diagnosis and treatment of pulmonary hypertension of the European Society of Cardiology (ESC) and the European Respiratory Society (ERS)". *Eur Respir J*. 2015;46:903–975. doi:10.1183/13993003.51032-2015
39. Vance SK, Imamura Y, Freund KB. The effects of sildenafil citrate on choroidal thickness as determined by enhanced depth imaging optical coherence tomography. *Retina*. 2011;31(2):332–335. doi:10.1097/IAE.0b013e3181eef0ae